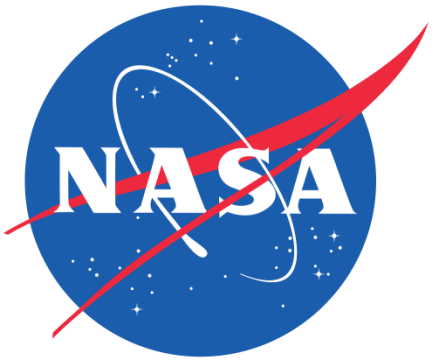

National Aeronautics and Space Administration
Langley Research Center

Stratospheric Aerosol and Gas Experiment on the International Space Station (SAGE III/ISS)

Data Products User's Guide

Version 6.0
Feb 2025

Change Record

Issue	Date	Sections Affected	Description
Version 1.0	Oct 2017	All	Baseline
Version 1.1	Dec 2017	Product Content and Formats, Appendices	Lunar information added
Version 2.0	Oct 2018	All	New data format
Version 3.0	Apr 2021	All	New data format
Version 5.21	July 2022	Appendix C; Minor Version Increment	Aer_width product clarification; minor version increment
Version 5.3	February 2023	All	New data format
Version 5.3 Patch 2	May 2024	Event Condition QA Flags	New QA flag
Version 6.0	Feb 2025	All	New data products and format

Contents

Acronyms and Abbreviations

ASDC	Atmospheric Sciences Data Center
ATBD	Algorithm Theoretical Basis Document
CCD	Charge-Coupled Device
Ch	Channel
DMP	Disturbance Monitoring Package
EFOV	Effective Field of View
EOS	Earth Observing System
ETOS	Elapsed Time on Station
EVA	Extravehicular Activity
FOV	Field of View
GAMS	Gas and Aerosol Measurement Sensor
GMAO	Global Modeling and Assimilation Office
HDF	Hierarchical Data Format
IFOV	Instantaneous Field of View
InGaAs	Indium Gallium Arsenide
IR	Infrared
ISS	International Space Station
LOS	Line of Sight
MERRA-2	Modern-Era Retrospective analysis for Research and Applications, Version 2
QA	Quality Assurance
SAGE	Stratospheric Aerosol and Gas Experiment
SAM	Stratospheric Aerosol Measurement
SCF	Science Computing Facility
SP	Slant Path

Information for using the SAGE III/ISS Data Product User's Guide

This Data Products User's Guide (Version 6.0) provides a general description of the measurement technique, instrument, mission, and sampling coverage. Additional information on these topics or details on the retrieval algorithms are provided at the websites specified below. This document also provides information on the CCD pixel assignments used for the retrieval algorithms. These assignments and the periods they represent are described in Appendix A. Instructions for accessing the SAGE III/ISS Data Product files are also provided, with detailed descriptions of their content and format given in Appendices B, C, and D.

Reference Material	Website Location
SAGE III Algorithm Theoretical Basis Documents	https://eospso.gsfc.nasa.gov/atbd-category/50
SAGE III/ISS Mission Web Site	https://sage.nasa.gov/

Introduction

The Stratospheric Aerosol and Gas Experiment on the International Space Station (SAGE III/ISS) is an extension of the successful SAM II, SAGE I, SAGE II, and SAGE III Meteor-3M satellite experiments and is designed to acquire measurements of aerosols and gases in the stratosphere and upper troposphere (Chu and Veiga). These measurements are needed to enhance our understanding of natural and human-derived atmospheric processes. The experiment is a component of NASA's Earth Observing System (EOS) and is mounted on the ISS. The mission is managed by NASA's Langley Research Center.

The design for the SAGE III instruments included some advances which permit measurement of additional wavelengths over SAGE II. These added measurement capabilities resulted in

- improved aerosol characterization,
- improved gaseous retrievals of O_3, H_2O, and NO_2,
- extended vertical range of measurements,
- self-calibration of the instrument, independent of external data, and
- expanded sampling coverage.

Measurement Technique

The SAGE III instrument measures the attenuation of solar radiation resulting from the scattering and absorption by constituents in the Earth's atmosphere as the spacecraft observes a sunrise or sunset event.

The viewing geometry of the satellite and the radiant target (Sun or Moon) during an occultation is illustrated in Figure 1. Measurement opportunities occur when the satellite ascends or descends from behind the Earth. Measurement begins when the instrument acquires the radiant target and uses a mirror to scan the target image, in the local vertical direction, across the instrument field-of-view (FOV) aperture. A measurement is considered to occur at the point along the line of sight from the instrument to the target that comes closest to the Earth's surface (i.e., the subtangent point). The altitude of that point above the Earth's surface is commonly referred to as the tangent altitude.

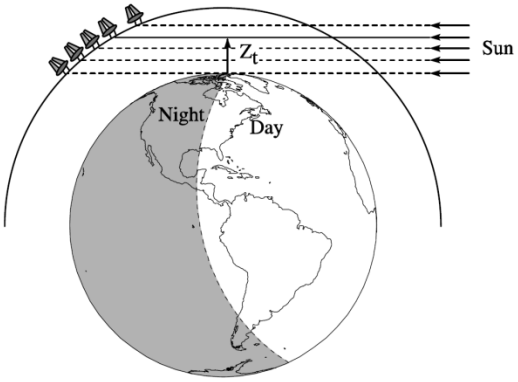

Figure 1. Occultation Geometry

The use of a scanning mirror provides multiple samples at each tangent altitude that are combined to construct transmission profiles from the Earth's surface (or cloud top) to an altitude of 100 km. Above this altitude, irradiance measurements are acquired between 100 and 300 km to characterize the instrument's performance across its wavelength range. This information is used to calibrate the instrument for each solar occultation event. By using this procedure, SAGE III data are relatively unaffected by changes in the instrument characteristics over the lifetime of the mission. A general description of the solar occultation measurement technique is provided by McCormick et al., 1979 (McCormick, Hamill and Pepin).

The atmospheric extinction at any point along the line-of-sight typically includes contributions from aerosols and several gas constituents. Figure 2 illustrates the principal extinction contributions for an altitude of 18 km. Both aerosol and molecular (Rayleigh)

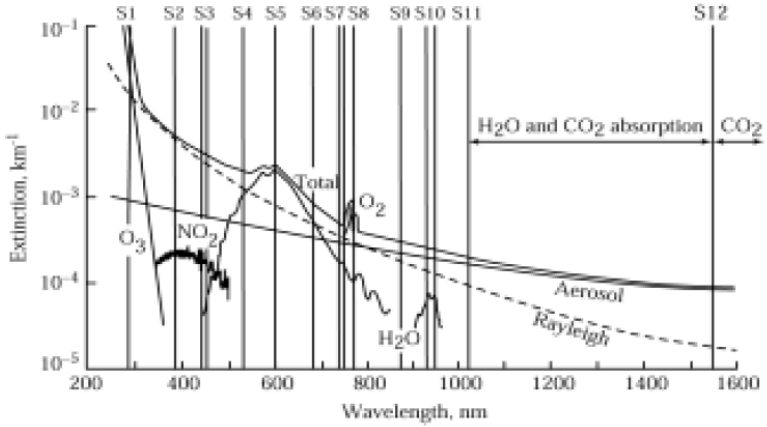

Ch #	Start-End WL (nm)	Target Species
01	284-296	O_3
02	382-387	Aerosol
03	433-451	NO_2/Aerosol
04	518-523	Aerosol
05	560-623	O_3/Aerosol
06	673-678	Aerosol
07	753-758	Aerosol
08	758-771	O_2
09	867-872	Aerosol
10	920-970	H_2O
11	1019-1025	Aerosol
12	1530-1560	Aerosol

Figure 2. Principal Extinction Contributions at 18 km
Vertical lines (S1-S12) denote spectral bands measured during solar events by SAGE III.

scattering contribute to extinction at all wavelengths. Ozone has strong absorption in the Hartley-Huggins band in the ultraviolet region of the spectrum and in the Chappuis band in the visible spectrum. NO_2 absorbs between 350 and 600 nm. Water vapor has absorption lines throughout the visible spectrum, with an additional strong band near 940 nm. Although they are not depicted in this figure, NO_3 has absorption features between 500 and 650 nm, and OClO has a strong band between 380 and 400 nm.

Instrument Description and Operation

The design of the SAGE III sensor relies heavily upon the flight-proven designs used in the SAM II and SAGE I and II instruments. The SAGE III sensor assembly is illustrated in Figure 3. It consists of a pointing subsystem, an imaging subsystem, and a spectrometer. The pointing subsystem uses a scan mirror to acquire radiant energy from either the Sun or the Moon by vertically scanning across the target's image. The imaging subsystem produces a focused image of the target at the focal plane where the science aperture is located. The aperture defines the instrument's instantaneous field of view (IFOV). A removable neutral-density filter is located along the optical path of this subsystem. The filter is inserted into the optical path to attenuate the solar signal by approximately a factor of 106 and is removed for lunar measurements.

The spectrometer is located behind the science aperture and uses an 809 × 11 pixel CCD array to measure target radiation. The solar radiance between 280 and 1040 nm is measured with a spectral resolution of 1 to 2 nm along the 809 pixel dimension. An additional InGaAs infrared (IR) photodiode measures light near 1550 nm with a bandwidth of 30 nm for near infrared aerosol extinction measurements. This spectral coverage permits the measurement of multiple absorption features of each gaseous species and multiwavelength measurements of broadband extinction by aerosols. Because of limitations in the telemetry bandwidth, only 87 pixel groups (86 from the CCD and 1 from the photodiode) are transmitted from the

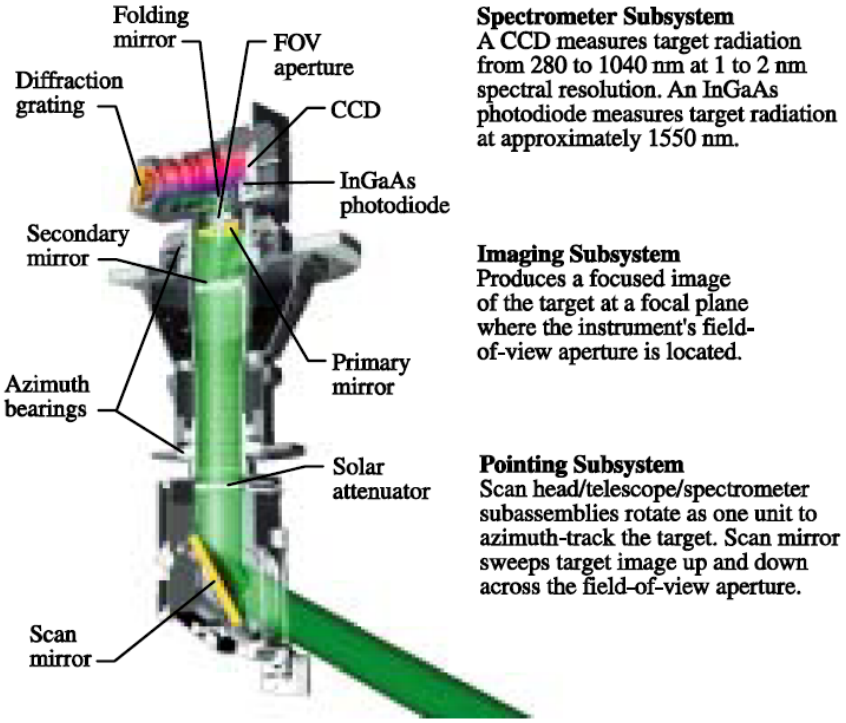

Figure 3. SAGE III Sensor Subsystems

satellite for solar occultations. These pixel groups are divided among 12 channels for solar observations and 3 channels for lunar observations. One of the features of the SAGE III/ISS instrument is the ability to reassign CCD pixels among these channels during flight to optimize instrument and retrieval performance. A listing of the different pixel assignments is provided in Appendix A.

As noted above, the CCD has 11 pixels along the horizontal direction for each of the 809 wavelength segments. The number of pixels utilized, consequently, defines the effective field of view (EFOV) in the horizontal direction. For solar measurements, 5 of the pixels are coadded, which results in an EFOV of 2.3 arc-min in the horizontal, and read out to produce data at an effect rate of 64 samples per second. With an instantaneous field of view of 0.5 arc-min in the vertical, a vertical scan rate of 15 arc-min/sec from an orbital altitude of 400 km results in a vertical resolution of 0.5 km and a horizontal resolution of 1.5 km at the tangent point location.

For lunar measurements, the measurement integration time is increased, the sample rate is decreased to 16 samples per second, and the EFOV is widened to include all 11 elements of the CCD to improve the measurement's signal-to-noise ratio. The increased integration time results in an increase in the EFOV to 1.5 arc-min in the vertical (or 1.0 km at the tangent point). The use of all 11 pixels increases the horizontal view to 5 arc-min (or 3.3 km at the tangent point).

SAGE III/ISS Mission

The SAGE III/ISS mission is a joint research experiment between NASA, the European

Space Agency (ESA), Thales Alenia Space-Italia (TAS-I), and Ball Aerospace & Technologies Corp. (BATC) (Szatkowski, Bradley Jr and Mauldin III). The instrument was launched as part of a resupply mission to the ISS on February 19, 2017. The ISS travels in a Low-Earth orbit at a variable altitude of 330-435 km at an inclination of 51.6°. With these orbital parameters, solar occultation measurement opportunities cover a large range of latitudes (between 70° S and 70° N). Solar observations are limited by beta angles in the range of -60° to +60°. Nominal sampling coverage for this mission is shown in Figure 4.

Additionally, observations are limited by ISS component obstructions, visiting vehicles, ISS maneuvers, and extravehicular activity (EVA, i.e., spacewalks). Lastly, onboard ISS activities occasionally cause vibrations that may increase the uncertainty of observations; although a pointing correction is made based on data from the Disturbance Monitoring Package (DMP). More information on the use of the DMP is provided in Hill, et al. (2022).

Data Products and Availability

A list of the profile measurements contained in the SAGE III/ISS science data products is provided in Table 1. The reporting interval for all species is 0.5 km. These data products, with attendant metadata, are archived and available in HDF5, binary format, and netCDF from the Atmospheric Science Data Center (ASDC).

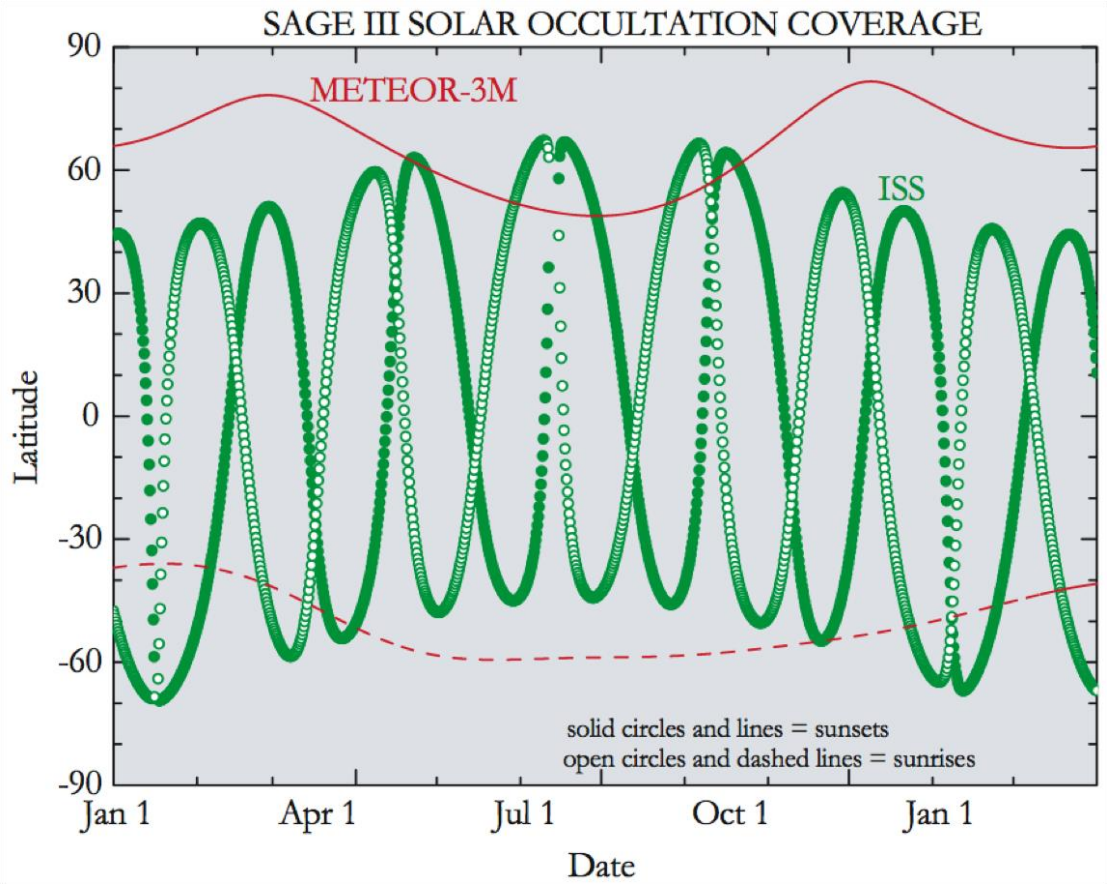

Figure 4. Nominal SAGE III/ISS Coverage Compared to SAGE III Meteor-3M Coverage

Table 1. SAGE III Measurement Inventory

Reported Measurement	Status*	Units	Vertical Range	Mid/Lower Stratosphere Precision	Product Residence
Transmission Slant Path Transmission	Validated Stage 1	none	0 - 100 km	0.05%	Level 1B Transmission
Aerosol (9 spectral bands) Extinction Coefficient	Validated Stage 1	km^{-1}	0 - 45 km	8%	Level 2 Solar
Ozone (MLR) Concentration	Validated Stage 2	cm^{-3}	0 - 70 km	5%	Level 2 Solar
Ozone (AO3) Concentration	Validated Stage 2	cm^{-3}	0 - 70 km	5%	Level 2 Solar
Ozone (Mesospheric) Concentration	Provisional	cm^{-3}	50 - 100 km	10%	Level 2 Solar
NO_2 Concentration	Validated Stage 2	cm^{-3}	0 - 70 km	15%	Level 2 Solar
Water Vapor Concentration	Validated Stage 2	cm^{-3}	0 - 60 km	20%	Level 2 Solar
Ozone Concentration	Validated Stage 1	cm^{-3}	0 - 70 km	10%	Level 2 Lunar
NO_2 Concentration	Provisional	cm^{-3}	0 - 70 km	10%	Level 2 Lunar
NO_3 Concentration	Provisional	cm^{-3}	0 - 70 km	10%	Level 2 Lunar

* Release Status Definitions
Validated Stage 2 – Product uncertainty is estimated over a significant set of locations/time periods by comparison with suitable reference data. Results are published in the peer-reviewed literature.
Validated Stage 1 – Product uncertainty is estimated using a small number of independent measurements obtained from suitable reference data.
Provisional – These data are partially validated and improvements are continuing; quality may not be optimal since validation and quality assurance are ongoing.
Research – Suitable for validation, potentially usable for science and publication. Users cautioned.
Beta – Products intended to enable users to gain familiarity with the parameters and the data. Comment to the SAGE III team is appreciated.

Data products are organized into individual solar or lunar event files and monthly solar or lunar files. This arrangement allows the user to select Level 1B and Level 2 products based on specified periods of time and measurement locations. SAGE III/ISS product files may be requested through the ASDC at any time.

Product Content and Formats

This section provides a description of the content and format for the HDF5 and binary Level 1B and Level 2 data products. The data formats for all binary product files are listed in detail in Appendices B, C, and D. This section also provides a description of the file-naming convention.

Reader software for SAGE III/ISS binary product files is available for download from

the ASDC website. These readers are currently available for the IDL and Python programming languages. Readers are not provided for the SAGE III/ISS HDF product files. Due to changes in data format between versions, the latest readers are required for the latest data product version.

Level 1B Transmission Product

The Level 1B Transmission product contains the SAGE III/ISS atmospheric slant path transmission profiles at 87 spectral channels, as listed in Appendix B. The profiles are skewed vertically and extend from sea level to an altitude of 100 km in 0.5 km intervals. The standard deviation of the binned transmission data is also provided for each reported altitude and channel. These datasets have been geolocated and normalized against exoatmospheric solar measurements to produce slant path transmission profiles. Algorithm retrievals outlined in the Algorithm Theoretical Basis Document (ATBD) are used to reduce and invert this data into the Level 2 products listed in Appendix C. The Level 1B product is only available for solar measurements.

In the construction of the transmission profiles, atmospheric density information is used to correct for refraction effects. This information is derived from temperature profiles interpolated to the location and time of each SAGE III/ISS event from global gridded meteorological analyses provided by NASA GMAO's MERRA-2. These data sets extend from the surface to a pressure-altitude around 0.01 hPa (~80 km). Above this altitude, climatological temperature data are used from GRAM95. The composite temperature profile information is included in the Level 1B and Level 2 data product.

Level 2 Solar Species Products

The Level 2 Solar Species products are produced from the Level 1B Transmission profiles by using algorithms described in the ATBD. Gas absorption data sources are identified in Appendix E. A description of the Level 2 Solar Species format is provided in Appendix C. This section discusses the content of the Level 2 Solar Species organized by species. Each species includes information on its relative uncertainty. Species are reported in profiles on a geometric altitude coordinate system with a vertical resolution of 0.5 km. Diurnal corrections, to compensate for rapid photochemistry across the terminator in the line-of-sight, are not applied to the retrieved constituent values.

Aerosol

Profiles of aerosol extinction at 9 wavelengths are provided from the surface, or opaque cloud top, to an altitude of 55 km, where the contribution due to aerosols becomes negligible at all wavelengths. In practice, the lower altitude of an aerosol extinction profile may be limited by the dynamic range of the detector and a high, integrated slant path optical depth.

Nitrogen Dioxide

Profiles of nitrogen dioxide are provided in units of concentration over the altitude range 0 to 100 km. These profile measurements are derived from the multiple linear regression retrieval algorithm as described in the ATBD.

Ozone

Three different profiles of ozone are provided in units of concentration over the altitude range 0 to 100 km. One profile is based upon measurements made at short wavelengths in the Hartley-Huggins band (denoted Mesospheric Ozone), a second profile is based upon measurements made at visible wavelengths in the Chappuis band (denoted MLR Ozone), and a third profile is obtained using a similar approach utilized to process

SAGE II data (denoted AO3 Ozone). Product files also include a generic "o3" profile intended for a future blend of these retrievals; for V6.0 it is a copy of the "AO3 Ozone" profile as the recommended profile for use.

Water Vapor

Profiles of water vapor are provided in units of concentration over the altitude range 0 to 60 km. The water vapor products are retrieved by using a nonlinear least-squares approach from the solar occultation measurements of spectral slant path transmission.

Level 2 Solar Derived Products

New data products have been added to the Level 2 solar files. These products are focused on aerosols, derived from the primary aerosol extinction coefficient profiles, and are broadly labeled: aerosol flag and aerosol particle size distribution. Both products were publicly available during 2024 as separate files but are now incorporated into the Level 2 solar files for simplicity and completeness.

Aerosol Flag

The development of this SAGE III/ISS Level 2 aerosol flag follows methods supporting a cloud-free aerosol product for the Global Space-based Stratospheric Aerosol Climatology (GloSSAC), in which SAGE III/ISS data plays a crucial role alongside other space-based measurements (Thomason et al., 2018; Kovilakam et al., 2020). A detailed description of the methods used in the aerosol categorization algorithm is available in Kovilakam et al. (2023). A modification is the use of additional screening. The screening relies on the count of negative extinction values and positive extinction values with an error exceeding 50%. If the number of negative and positive extinction values with an error greater than 50% exceeds a third of the total number of extinction data points between the tropopause and 25 km altitude, the respective profile is discarded for categorization and labeled as "Transmission Anomaly". Consequently, several aerosol flag profiles might be absent when compared to the Level 2 extinction data. Additionally, tropopause height is revisited for the Level 2 aerosol flag product. An accurate tropopause height is essential for the method, prompting a comparison between tropopause heights determined using the WMO method (e.g., BMO, 1992; Randel et al., 2000) and those reported in the primary Level 2 data. The higher of the two values is then adopted as the tropopause height for that event. Both values are included in the Level 2 solar data.

Aerosol Particle Size Distribution (PSD)

An evaluation of possible particle size distribution (PSD) consistent with the observed aerosol extinction coefficient spectra is performed using the method of Knepp et al. (2024), with no adjustments. The data included is listed in Table C1, notably various moments of the PSD and items germane to the retrieval.

Level 2 Lunar Species Products

The retrieval of constituent profiles from irradiance measurements acquired during lunar occultation events are more complex than those employed for solar events because they account for the spatial non-uniformity of the surface albedo of the moon and the much lower measurement signal. One important difference between the solar and lunar retrieval techniques is the absence of a Level 1B slant path transmission profile product for lunar occultation retrievals, a consequence of not being able to determine limb-darkening curves with sufficient accuracy to calibrate each lunar occultation event. The inaccuracies in the registration of the limb-darkening curve arise from small uncertainties in the pointing knowledge of the instrument in the presence

of large variations in albedo across the lunar surface.

As a result of these challenges, the retrieval of lunar Level 2 products uses a different approach than is used for solar. A multiple linear regression is performed on the spectrum of relative optical depth for each packet, with the species absorption cross sections evaluated as the independent variables. Gas absorption data sources are identified in Appendix E. The resulting slant-path column densities are then bin-averaged, onion peeled, and reported on a geometric coordinate system with a vertical resolution of 0.5 km to maintain grid spacing compatibility with the solar Level 2 products. The tangent height registration of data for lunar profiles is accomplished by two methods, an ephemeris-based calculation and a comparison to a forward model of the oxygen A-band. The offset between the two methods is reported in the product.

A description of the content of these products is provided below and organized by species. Each product includes information on its relative uncertainty and a data quality assurance flag set.

A description of the lunar data product format and content is provided in Appendix D.

Ozone

Profiles of ozone are provided in units of concentration from 0 to 100 km. Profile measurements are derived from the multiple linear regression retrieval algorithm used for GAMS described in Reference (Pitts, Thomason and Zawodny).

Nitrogen Trioxide

Profiles of nitrogen trioxide are provided in units of concentration from 0 to 100 km. Profile measurements are derived from the multiple linear regression retrieval algorithm used for GAMS described in Reference (Pitts, Thomason and Zawodny).

Nitrogen Dioxide

Profiles of nitrogen dioxide are provided in units of concentration from 0 to 100 km. Profile measurements are derived from the multiple linear regression retrieval algorithm used for GAMS described in Reference (Pitts, Thomason and Zawodny).

File-Naming Convention

Following is a list of products and the file-naming convention for each product that shall be generated by SAGE III/ISS SCF processing.

- **L1B Solar Transmission Binary Products:** g3b_tb_z.z.z_YYYYMMDDEETT.dat
- **L1B Solar Transmission HDF Products:** g3b_t_z.z.z_YYYYMMDDEETT.h5
- **Level 2 Solar Binary Products:** g3b_sspb_z.z.z_YYYYMMDDEETT.dat
- **Level 2 Solar HDF Products:** g3b_ssp_z.z.z_YYYYMMDDEETT.h5
- **Level 2 Lunar Binary Products:** g3b_lspb_z.z.z_YYYYMMDDEETT.dat
- **Level 2 Lunar HDF Products:** g3b_lsp_z.z.z_YYYYMMDDEETT.h5
- **L1B Monthly Solar Transmission NETCDF Products:** g3b_tmnc_z.z.z_YYYYMM.nc
- **Level 2 Monthly Solar NETCDF Products:** g3b_smnc_z.z.z_YYYYMM.nc
- **Level 2 Monthly Lunar NETCDF Products:** g3b_lmnc_z.z.z_YYYYMM.nc
- **where:**
    - YYYY=year
    - MM=month
    - DD=day of month
    - EE=event number of the day
    - TT=event type (SR = sunrise, SS = sunset, MR = moonrise, MS = moonset)
    - z.z.z = Data Product Version Number

Example: g3b_tb_6.0.0_2017060702SS.dat
Refers to a transmission binary file for SAGE III/ISS captured on June 7, 2017 during the second event of the day, which was a sunset, and released as a product of SCF Data Product Version 6.0.0.

Example: g3b_ssp_6.0.0_2017060703SR.h5
Refers to a solar HDF5 file for SAGE III/ISS captured on June 7, 2017 during the third event of the day, which was a sunrise, and released as a product of SCF Data Product Version 6.0.0.

Example: g3b_smnc_6.0.0_20170601.nc
Refers to a solar monthly NETCDF file for SAGE III/ISS capturing all solar events for June 2017 and released as a product of SCF Data Product Version 6.0.0.

Quality Assurance Flags

SAGE III Data Products are reviewed prior to their release. Profiles have values reported only for those species and altitudes where there is confidence in the ability of the algorithms to produce representative products. Each file contains flags that convey information about processing decisions to the user.

Calibration and Correction

For each event, a Boolean product is set to True when the following were applied:

Disturbance correction – DMP-based pointing correction was applied (solar only).

Wavelength calibration – Nominal CCD Pixel-wavelength mapping was adjusted based on fitting of exoatmospheric spectrum

Event Condition QA Flags

For each event, a Boolean product is set to True when the following conditions occur:

Hexapod error – Nadir pointing by the hexapod platform could not be achieved.

Contamination door closed – Instrument contamination door was closed.

Time questionable – Packet-time assignments were questionable.

Exoatmospheric disturbance – Large ISS vibrational disturbances were detected when collecting exoatmospheric data (solar only).

Exoatmospheric blockage – Obstruction of the target by an ISS element was detected when collecting exoatmospheric data (solar only).

Solar eclipse – The sun was obstructed by the moon (solar only).

Nadir drift – Scan head pointing drift greater than 1 degree off-nadir detected during event.

Thermal control fault – CCD temperature was outside control band during the event.

Ephemeris gaps – Gaps in ISS ephemeris were detected.

Altitude Dependent QA Flags

Each altitude bin is assigned several QA flags. A Boolean product is set to True when the following conditions occur:

Disturbance –Large ISS vibrational disturbances were detected when collecting data for this altitude bin. Only present for solar events.

Climatology used – Climatology meteorological parameters used for this altitude bin.

Interpolated data – Transmission data was interpolated for this altitude bin. Only present for solar events.

Solar Product Status and Quality

The data products have been screened by the SAGE III/ISS team in order to remove failed events and/or specific product profiles. Most of these are due to platform-related issues such as blockages and severe platform disturbances, but a few fail due to unknown instrument and/or retrieval algorithm anomalies. As a matter of practice, only the most severe failed events are removed and some thought into filtering data for less egregious data anomalies may be necessary for the user.

Ozone

The last time the "MLR" and "AO3" ozone products were thoroughly validated in a peer-reviewed publication was for v5.1 (Wang et al., 2020). The primary differences in v5.2 were the natural tradeoff between precision and vertical resolution when vertical smoothing was removed and the reduction in low-altitude biases from a correction in spectroscopy. This was followed by a slight reduction in random noise in v5.3. Updating the ozone spectroscopy to Gorshelev et al. (2014) and Serdyuchenko et al. (2014) results in ~2% more ozone in v6.0 compared to v5.3. While the MLR and AO3 profiles are generally in good agreement, the AO3 product has less noise in the upper stratosphere (above 40 km) and is thus the recommended ozone product. The SAGE III/ISS AO3 ozone data are of sufficient quality to be suitable for scientific research including trend studies.

The mesospheric (i.e., "Ozone_Mes") product is provisional status based on ACE-FTS comparisons though it is still affected by out-of-band stray light, which is corrected using an imperfect approach developed for SAGE III/M3M, resulting in biases that are most noticeable at the lower end of the retrieval range.

In the past, SAGE III has provided a composite ozone product. In V6.0 this product is set to the AO3 ozone. The SAGE Team feels additional thought into the construction of a blended product and implementation of improved corrections for the mesospheric ozone are required to have a more advanced product.

Aerosol Extinction Coefficient

The v5.2 aerosol extinction coefficient profiles were validated by Kalnajs and Deshler (2022). However, prior to that work the aerosol extinction coefficient products have already been used for a number of studies related to validation of other instruments (e.g., Kar et al., 2019; Rieger et al., 2019; Chen et al., 2020), documenting the impacts of recent volcanic eruptions and wildfires, and contributing to long-term studies of aerosol (e.g., Chouza et al., 2020; Kovilakam et al., 2020). Kalnajs & Deshler note the long-standing bias at 1um between SAGE and in-situ derived extinction. An additional anomaly was noted in the literature, namely a negative bias in the 520, 602, and 676 nm aerosol channels coinciding/scaling with the ozone cross-sections (illustrated in Wang et al., 2020). This bias has been reduced with the use of newer ozone absorption cross-sections noted in Appendix E. Finally, as noted by Wang et al. (2020) and Boone et al. (2024), the 756 nm aerosol channel has a slight, altitude dependent positive bias resulting from uncleared O_2 absorption, which will be corrected in a future version.

Nitrogen Dioxide

The v5.1 NO2 products have undergone some preliminary validation in Dube et al. (2020) and more extensive evaluation by Strode et al. (2022). The largest change between v5.1 and

v5.2 comes from the new wavelength map, resulting in a ~5% decrease in overall NO2 in the stratosphere.

Water Vapor

The last time the vertical profiles of H2O concentration were thoroughly validated in a peer-reviewed publication was for v5.1 in Davis et al. (2021) and Park et al. (2021), showing good agreement with other instruments as well as capturing patterns of stratospheric variability. Several anomalies noted in those studies were mitigated and/or improved in v5.2, most noticeable failed retrievals and enhanced sensitivity to elevated aerosol loading. Additionally, changes in the PSFs resulted in a roughly 0.3 ppm increase in stratospheric water vapor. With the combination of previous validation studies and improvements to the data, water vapor should be considered suitable for scientific studies from v5.2 onward.

Lunar Product Status and Quality

Ozone

The vertical profiles of ozone concentration have undergone some preliminary validation and the show generally good agreement with other instruments and the SAGE solar ozone product.

Nitrogen Dioxide

The vertical profiles of NO2 concentration are a provisional product with limited evaluation. While individual profiles have significant noise, averaging multiple profiles (e.g., over ~24 hours) to improve the precision shows lunar NO2 behaves similar to the solar NO2 product.

Nitrogen Trioxide

The vertical profiles of NO3 concentration are a provisional product with the user cautioned on the use of this data. This product tends to be rather noisy and, under most conditions, requires substantial averaging to produce a meaningful profile.

References

BMO: International Meteorological Vocabulary, WMO, World Meteorological Organization, URL https://library. wmo.int/records/item/35809-international-meteorological-vocabulary, 1992

Bogumil, K., et al. "Measurements of molecular absorption spectra with the SCIAMACHY pre-flight model: instrument characterization and reference data for atmospheric remote-sensing in the 230–2380 nm region." *Journal of Photochemistry and Photobiology A: Chemistry* 157.2-3 (2003): 167-184.

Boone, C.D., et al. "Sulfate aerosol properties derived from combining coincident ACE-FTS and SAGE III/ISS measurements." *Journal of Quantitative Spectroscopy and Radiative Transfer,* 312 (2024): 108815.

Bucholtz, A. "Rayleigh-scattering calculations for the terrestrial atmosphere." *Applied Optics* 34 (1995): 2765-2773.

Chen, Z., et al. "Evaluation of the OMPS/LP stratospheric aerosol extinction product using SAGE III/ISS observations." *Atmos. Meas. Tech.,* 13 (2020): 3471–3485.

Chouza, F., et al. "Long-term (1999–2019) variability of stratospheric aerosol over Mauna Loa, Hawaii, as seen by two co-located lidars and satellite measurements." *Atmos. Chem. Phys.,* 20 (2020): 6821–6839.

Chu, W.P. and R Veiga. "SAGE III/EOS." *SPIE, vol. 3501* (September 1998): 52-60.

Davis, S. M., et al. "Validation of SAGE III/ISS solar water vapor data with correlative satellite and balloon-borne measurements." *Journal of Geophysical Research: Atmospheres,* 126: (2021).

Dube, K., et al. "Accounting for the photochemical variation in stratospheric NO2 in the SAGE III/ISS solar occultation retrieval." *Atmos. Meas. Tech.,* 14 (2021): 557–566.

Gorshelev, V., et al. "High spectral resolution ozone absorption cross-sections – Part 1: Measurements, data analysis and comparison with previous measurements around 293 K", *Atmos. Meas. Tech.,* 7 (2014): 609–624.

Greenblatt, G.D., et al. "Absorption Measurements of Oxygen Between 330 and 1140 nm." *Journal of Geophysical Research* 95 (1990): 18577-18582.

Hill, Charles A., et al. *Utilization of Disturbance Monitoring Package in Data Products*. NASA Langley Research Center, Hampton, VA, USA, 13 October 2022. SAGE III/ISS Science Team Meeting. <https://sage.nasa.gov/wp/wp-content/uploads/2022/11/DMP.pdf>.

Kalnajs, L. E. and T. Deshler. "A new instrument for balloon-borne in situ aerosol size distribution measurements, the continuation of a 50 year record of stratospheric aerosols measurements." *Journal of Geophysical Research: Atmospheres,* 127 (2022): e2022JD037485.

Kar, J., et al. "CALIPSO level 3 stratospheric aerosol profile product: version 1.00 algorithm description and initial assessment." *Atmos. Meas. Tech.,* 12 (2019): 6173–6191.

Kloss, C., et al. "Stratospheric aerosol layer perturbation caused by the 2019 Raikoke and Ulawun eruptions and their radiative forcing." *Atmos. Chem. Phys.,* 21 (2021): 535–560.

Knepp, T. N., et al. "Characterization of stratospheric particle size distribution uncertainties using SAGE II and SAGE III/ISS extinction spectra", *Atmos. Meas. Tech.,* 17 (2024): 2025–2054.

Kovilakam, M., et al. "The Global Space-based Stratospheric Aerosol Climatology (version 2.0): 1979–2018." *Earth Syst. Sci. Data,* 12 (2020): 2607–2634.

Kovilakam, M., et al. "SAGE III/ISS aerosol/cloud categorization and its impact on GloSSAC", *Atmospheric Measurement Techniques*, 16 (2023): 2709–2731.
McCormick, M. P., et al. "Satellite Studies of the Stratospheric Aerosol." *BAMS,* 60 (September 1979): 1038-1046.
Park, M., et al. "Near-global variability of stratospheric water vapor observed by SAGE III/ISS." *Journal of Geophysical Research: Atmospheres,* 126 (2021): e2020JD034274.
Pitts, M.C, et al. "Ozone observations by the Gas and Aerosol Measurement Sensor during SOLVE II." *Atmos. Chem. Phys.* 6 (2006): 2695-2709.
Randel, W. J., et al. "Interannual variability of the tropical tropopause derived from radiosonde data and NCEP reanalyses", *Journal of Geophysical Research: Atmospheres*, 105 (2000): 15 509–15 523.
Rieger, L. A., et al. "A multiwavelength retrieval approach for improved OSIRIS aerosol extinction retrievals." *Journal of Geophysical Research: Atmospheres,* 124 (2019): 7286–7307.
Rothman, L.S., et al. "The HITRAN 2004 molecular spectroscopic database." *Journal of Quantitative Spectroscopy & Radiative Transfer* 96 (2005): 139-204.
Serdyuchenko, A., et al. "High spectral resolution ozone absorption cross-sections – Part 2: Temperature dependence", *Atmos. Meas. Tech.*, 7 (2014): 625–636.
Strode, S. A., et al. "SAGE III/ISS ozone and NO2 validation using diurnal scaling factors." *Atmos. Meas. Tech.,* 15 (2022): 6145–6161.
Szatkowski, L., et al. "Stratospheric Aerosol and Gas Experiment III (SAGE III) Mission aboard the International Space Station." *SPIE, vol.3756* (July 1999): 164-169.
Thomason, L. W., et al. "A global space-based stratospheric aerosol climatology: 1979–2016", *Earth System Science Data*, 10 (2018): 469–492.
Wang, H. J. R., et al. "Validation of SAGE III/ISS solar occultation ozone products with correlative satellite and ground based measurements." *Journal of Geophysical Research: Atmospheres,* 125 (2020): e2020JD032430.
Yokelson, R.J., et al. "Temperature Dependence of the NO3 Absorption Spectrum." *Journal of Physical Chemistry* 98 (1994): 13144-13150.

Appendix A. SAGE III/ISS Nominal CCD Pixel Assignments

Table A1. Nominal CCD Assignments for Solar Data Collection (CCD Table Version 4)

Science Pixel Group	CCD Start Pixel	CCD End Pixel	Pixel Group Center Wavelength	Comment
0	2	2	281.916	
1	3	10	286.124	8-pixel sum
2	11	17	293.138	7-pixel sum
3	109	113	384.12	5-pixel average
4	163	163	433.091	
5	164	164	434.034	
6	165	165	434.977	
7	166	166	435.921	
8	167	167	436.864	
9	168	168	437.807	
10	169	169	438.751	
11	170	170	439.694	
12	171	171	440.637	
13	172	172	441.581	
14	173	173	442.525	
15	174	174	443.468	
16	175	175	444.412	
17	176	176	445.356	
18	177	177	446.299	
19	178	178	447.243	
20	179	179	448.187	
21	180	180	449.131	
22	181	181	450.075	
23	254	258	520.504	5-pixel average
24	299	301	562.042	3-pixel sum
25	306	308	568.648	3-pixel sum

Science Pixel Group	CCD Start Pixel	CCD End Pixel	Pixel Group Center Wavelength	Comment
26	313	315	575.255	3-pixel sum
27	320	322	581.861	3-pixel sum
28	327	329	588.466	3-pixel sum
29	334	336	595.071	3-pixel sum
30	341	343	601.674	3-pixel sum
31	348	350	608.277	3-pixel sum
32	355	357	614.879	3-pixel sum
33	362	364	621.481	3-pixel sum
34	419	423	676.133	5-pixel average
35	504	508	756.037	5-pixel average
36	509	509	758.852	
37	510	510	759.79	
38	511	511	760.728	
39	512	512	761.666	
40	513	513	762.604	
41	514	514	763.542	
42	515	515	764.48	
43	516	516	765.418	
44	517	517	766.356	
45	518	518	767.294	
46	519	519	768.232	
47	520	520	769.169	
48	521	521	770.107	
49	522	522	771.045	
50	625	629	869.207	5-pixel average
51	682	682	920.354	
52	696	696	933.339	
53	697	697	934.266	

Science Pixel Group	CCD Start Pixel	CCD End Pixel	Pixel Group Center Wavelength	Comment
54	698	698	935.193	
55	699	699	936.12	
56	700	700	937.046	
57	701	701	937.973	
58	702	702	938.9	
59	703	703	939.826	
60	704	704	940.752	
61	705	705	941.679	
62	706	706	942.605	
63	707	707	943.531	
64	708	708	944.457	
65	709	709	945.383	
66	710	710	946.309	
67	711	711	947.235	
68	712	712	948.161	
69	713	713	949.086	
70	714	714	950.012	
71	715	715	950.937	
72	716	716	951.863	
73	717	717	952.788	
74	718	718	953.714	
75	719	719	954.639	
76	720	720	955.564	
77	721	721	956.489	
78	722	722	957.414	
79	737	737	971.279	
80	789	789	1019.19	
81	790	790	1020.11	

Science Pixel Group	CCD Start Pixel	CCD End Pixel	Pixel Group Center Wavelength	Comment
82	791	791	1021.03	
83	792	792	1021.95	
84	793	793	1022.87	
85	794	794	1023.79	
86	-	-	1543.76	Photodiode

Table A2. Nominal CCD Assignments for Lunar Data Collection (CCD Table Version 2)

Science Pixel Group	CCD Start Pixel	CCD End Pixel	Pixel Group Center Wavelength	Comment
0	105	105	378.478	
1	106	106	379.418	
2	107	107	380.358	
3	108	108	381.298	
4	109	109	382.239	
5	110	110	383.179	
6	111	111	384.119	
7	112	112	385.06	
8	113	113	386	
9	114	114	386.941	
10	115	115	387.882	
11	116	116	388.822	
12	117	117	389.763	
13	118	118	390.704	
14	119	119	391.645	
15	120	120	392.585	
16	121	121	393.526	
17	122	122	394.467	
18	123	123	395.408	
19	124	124	396.349	
20	125	125	397.291	
21	126	126	398.232	
22	127	127	399.173	
23	128	128	400.114	
24	129	129	401.056	
25	130	130	401.997	
26	131	131	402.938	

Science Pixel Group	CCD Start Pixel	CCD End Pixel	Pixel Group Center Wavelength	Comment
27	132	132	403.88	
28	133	133	404.821	
29	144	144	415.182	
30	145	145	416.124	
31	146	146	417.066	
32	147	147	418.008	
33	148	148	418.95	
34	149	149	419.893	
35	150	150	420.835	
36	151	151	421.778	
37	152	152	422.72	
38	153	153	423.663	
39	154	154	424.605	
40	155	155	425.548	
41	156	156	426.491	
42	157	157	427.433	
43	158	158	428.376	
44	159	159	429.319	
45	160	160	430.262	
46	161	161	431.205	
47	162	162	432.148	
48	163	163	433.091	
49	164	164	434.034	
50	165	165	434.977	
51	166	166	435.921	
52	167	167	436.864	
53	168	168	437.807	
54	169	169	438.751	

Science Pixel Group	CCD Start Pixel	CCD End Pixel	Pixel Group Center Wavelength	Comment
55	170	170	439.694	
56	171	171	440.637	
57	172	172	441.581	
58	173	173	442.525	
59	174	174	443.468	
60	175	175	444.412	
61	176	176	445.356	
62	177	177	446.299	
63	178	178	447.243	
64	179	179	448.187	
65	180	180	449.131	
66	181	181	450.075	
67	182	182	451.019	
68	183	183	451.963	
69	184	184	452.907	
70	185	185	453.852	
71	186	186	454.796	
72	187	187	455.74	
73	188	188	456.684	
74	189	189	457.629	
75	190	190	458.573	
76	191	191	459.518	
77	192	192	460.462	
78	193	193	461.407	
79	194	194	462.352	
80	195	195	463.296	
81	196	196	464.241	
82	197	197	465.186	

Science Pixel Group	CCD Start Pixel	CCD End Pixel	Pixel Group Center Wavelength	Comment
83	198	198	466.131	
84	199	199	467.076	
85	200	200	468.021	
86	201	201	468.966	
87	202	202	469.911	
88	203	203	470.856	
89	204	204	471.801	
90	205	205	472.746	
91	206	206	473.691	
92	207	207	474.637	
93	208	208	475.582	
94	209	209	476.527	
95	210	210	477.473	
96	211	211	478.418	
97	212	212	479.364	
98	213	213	480.31	
99	214	214	481.255	
100	215	215	482.201	
101	216	216	483.147	
102	217	217	484.093	
103	218	218	485.039	
104	219	219	485.984	
105	220	220	486.93	
106	221	221	487.876	
107	222	222	488.823	
108	233	233	498.789	
109	234	234	499.733	
110	235	235	500.677	

Science Pixel Group	CCD Start Pixel	CCD End Pixel	Pixel Group Center Wavelength	Comment
111	236	236	501.621	
112	237	237	502.565	
113	238	238	503.509	
114	239	239	504.453	
115	240	240	505.398	
116	241	241	506.342	
117	242	242	507.286	
118	243	243	508.23	
119	244	244	509.174	
120	245	245	510.118	
121	246	246	511.062	
122	247	247	512.007	
123	248	248	512.951	
124	249	249	513.895	
125	250	250	514.839	
126	251	251	515.783	
127	252	252	516.727	
128	253	253	517.672	
129	254	254	518.616	
130	255	255	519.56	
131	256	256	520.504	
132	257	257	521.448	
133	258	258	522.392	
134	259	259	523.336	
135	260	260	524.28	
136	261	261	525.225	
137	262	262	526.169	
138	263	263	527.113	

Science Pixel Group	CCD Start Pixel	CCD End Pixel	Pixel Group Center Wavelength	Comment
139	264	264	528.057	
140	265	265	529.001	
141	266	266	529.945	
142	267	267	530.889	
143	268	268	531.833	
144	269	269	532.777	
145	270	270	533.722	
146	271	271	534.666	
147	272	272	535.61	
148	273	273	536.554	
149	274	274	537.498	
150	275	275	538.442	
151	276	276	539.386	
152	277	277	540.33	
153	278	278	541.274	
154	279	279	542.218	
155	280	280	543.162	
156	281	281	544.106	
157	282	282	545.05	
158	283	283	545.994	
159	284	284	546.938	
160	285	285	547.882	
161	292	292	554.49	
162	293	293	555.434	
163	294	294	556.378	
164	295	295	557.322	
165	296	296	558.266	
166	297	297	559.21	

Science Pixel Group	CCD Start Pixel	CCD End Pixel	Pixel Group Center Wavelength	Comment
167	298	298	560.154	
168	299	299	561.098	
169	300	300	562.042	
170	301	301	562.985	
171	302	302	563.929	
172	303	303	564.873	
173	304	304	565.817	
174	305	305	566.761	
175	306	306	567.705	
176	307	307	568.649	
177	308	308	569.592	
178	309	309	570.536	
179	310	310	571.48	
180	311	311	572.424	
181	312	312	573.367	
182	313	313	574.311	
183	314	314	575.255	
184	315	315	576.199	
185	316	316	577.142	
186	317	317	578.086	
187	318	318	579.03	
188	319	319	579.974	
189	320	320	580.917	
190	321	321	581.861	
191	322	322	582.805	
192	323	323	583.748	
193	324	324	584.692	
194	325	325	585.635	

Science Pixel Group	CCD Start Pixel	CCD End Pixel	Pixel Group Center Wavelength	Comment
195	326	326	586.579	
196	327	327	587.522	
197	328	328	588.466	
198	329	329	589.41	
199	330	330	590.353	
200	331	331	591.297	
201	332	332	592.24	
202	333	333	593.184	
203	334	334	594.127	
204	335	335	595.071	
205	336	336	596.014	
206	337	337	596.957	
207	338	338	597.901	
208	339	339	598.844	
209	340	340	599.788	
210	341	341	600.731	
211	342	342	601.674	
212	343	343	602.618	
213	344	344	603.561	
214	345	345	604.504	
215	346	346	605.448	
216	347	347	606.391	
217	348	348	607.334	
218	349	349	608.277	
219	350	350	609.221	
220	351	351	610.164	
221	352	352	611.107	
222	353	353	612.05	

Science Pixel Group	CCD Start Pixel	CCD End Pixel	Pixel Group Center Wavelength	Comment
223	354	354	612.993	
224	355	355	613.936	
225	356	356	614.879	
226	357	357	615.823	
227	358	358	616.766	
228	359	359	617.709	
229	360	360	618.652	
230	361	361	619.595	
231	362	362	620.538	
232	363	363	621.481	
233	364	364	622.424	
234	365	365	623.366	
235	366	366	624.309	
236	367	367	625.252	
237	368	368	626.195	
238	369	369	627.138	
239	370	370	628.081	
240	371	371	629.024	
241	372	372	629.966	
242	373	373	630.909	
243	374	374	631.852	
244	375	375	632.795	
245	376	376	633.737	
246	377	377	634.68	
247	378	378	635.623	
248	379	379	636.565	
249	380	380	637.508	
250	381	381	638.45	

Science Pixel Group	CCD Start Pixel	CCD End Pixel	Pixel Group Center Wavelength	Comment
251	382	382	639.393	
252	383	383	640.336	
253	384	384	641.278	
254	385	385	642.221	
255	386	386	643.163	
256	387	387	644.105	
257	388	388	645.048	
258	389	389	645.99	
259	390	390	646.933	
260	391	391	647.875	
261	392	392	648.817	
262	393	393	649.76	
263	394	394	650.702	
264	395	395	651.644	
265	396	396	652.586	
266	397	397	653.528	
267	398	398	654.471	
268	399	399	655.413	
269	400	400	656.355	
270	401	401	657.297	
271	402	402	658.239	
272	403	403	659.181	
273	404	404	660.123	
274	405	405	661.065	
275	406	406	662.007	
276	407	407	662.949	
277	408	408	663.891	
278	409	409	664.833	

Science Pixel Group	CCD Start Pixel	CCD End Pixel	Pixel Group Center Wavelength	Comment
279	410	410	665.775	
280	411	411	666.716	
281	412	412	667.658	
282	413	413	668.6	
283	414	414	669.542	
284	415	415	670.483	
285	416	416	671.425	
286	417	417	672.367	
287	418	418	673.308	
288	419	419	674.25	
289	420	420	675.191	
290	421	421	676.133	
291	422	422	677.074	
292	423	423	678.016	
293	424	424	678.957	
294	425	425	679.899	
295	426	426	680.84	
296	427	427	681.781	
297	428	428	682.723	
298	429	429	683.664	
299	430	430	684.605	
300	431	431	685.547	
301	432	432	686.488	
302	433	433	687.429	
303	434	434	688.37	
304	435	435	689.311	
305	436	436	690.252	
306	437	437	691.193	

Science Pixel Group	CCD Start Pixel	CCD End Pixel	Pixel Group Center Wavelength	Comment
307	438	438	692.134	
308	439	439	693.075	
309	440	440	694.016	
310	441	441	694.957	
311	442	442	695.898	
312	443	443	696.839	
313	505	506	755.568	2-pixel average
314	507	508	757.444	2-pixel average
315	509	509	758.852	
316	510	510	759.79	
317	511	511	760.728	
318	512	512	761.666	
319	513	513	762.604	
320	514	514	763.542	
321	515	515	764.48	
322	516	516	765.418	
323	517	517	766.356	
324	518	518	767.294	
325	519	519	768.232	
326	520	520	769.169	
327	521	521	770.107	
328	522	522	771.045	
329	523	523	771.982	
330	524	524	772.92	
331	525	525	773.858	
332	526	526	774.795	
333	527	527	775.732	
334	528	528	776.67	

Science Pixel Group	CCD Start Pixel	CCD End Pixel	Pixel Group Center Wavelength	Comment
335	529	529	777.607	
336	530	530	778.544	
337	531	531	779.482	

Appendix B. SAGE III/ISS Level 1B Solar Transmission Products

Table B1. Binary File Format Sheet: SAGE III/ISS Level 1B Solar Transmission Product

End Byte	Num Values	Dimension	Data Type	Product	Unit
3	3	3	str	mission_id	*
19	16	16	str	product_id	*
35	16	16	str	product_version	*
47	12	12	str	event_id	*
49	2	2	str	spacecraft_event_type	*
51	2	2	str	ground_event_type	*
67	16	16	str	datetime	*
75	1	1	float64	year_fraction	*
79	1	1	int32	int32_fill	*
83	1	1	float32	float32_fill	*
91	1	1	float64	float64_fill	*
95	1	1	float32	latitude	degrees
99	1	1	float32	longitude	degrees
103	1	1	float32	solar_beta	degrees
107	1	1	int32	n_ground_track_altitudes	*
151	11	11	float32	ground_track_altitude	km
327	176	176	str	ground_track_datetime	*
371	11	11	float32	ground_track_latitude	degrees
415	11	11	float32	ground_track_longitude	degrees
459	11	11	float32	ground_track_ray_direction	degrees
503	11	11	float32	spacecraft_latitude	degrees
547	11	11	float32	spacecraft_longitude	degrees
591	11	11	float32	spacecraft_altitude	km
595	1	1	int32	n_altitudes	*
1395	200	200	float32	altitude	km
2195	200	200	float32	geopotential_altitude	km

2196	1	1	bool	contamination_door_closed	*
2197	1	1	bool	solar_eclipse	*
2198	1	1	bool	hexapod_error	*
2199	1	1	bool	nadir_drift	*
2200	1	1	bool	time_questionable	*
2201	1	1	bool	exoatmospheric_blockage	*
2202	1	1	bool	exoatmospheric_disturbance	*
2203	1	1	bool	thermal_control_fault	*
2204	1	1	bool	ephemeris_gaps	*
2404	200	200	bool	disturbance	*
2405	1	1	bool	disturbance_correction	*
2409	1	1	int32	ccd_version	*
2410	1	1	bool	wavelength_calibration	*
2414	1	1	float32	wavelength_shift	nm
2418	1	1	float32	wavelength_stretch	nm/pixel
2422	1	1	float32	ccd_temperature	deg C
2426	1	1	float32	ccd_temperature_deviation	deg C
2430	1	1	float32	ccd_shield_temperature	deg C
2434	1	1	float32	spectrometer_zenith_temperature	deg C
2466	32	32	str	climatology_source	*
2498	32	32	str	met_source	*
3298	200	200	float32	temperature	K
4098	200	200	float32	pressure	hPa
4898	200	200	float32	neutral_density	cm^{-3}
5098	200	200	bool	climatology_used	*
5102	1	1	float32	tropopause_altitude	km
5106	1	1	float32	tropopause_pressure	hPa
5110	1	1	float32	tropopause_temperature	K
5114	1	1	int32	n_pixel_groups	*
5462	87	87	float32	wavelength	nm

5810	87	87	float32	nominal_wavelength	nm
5814	1	1	float32	sunspot_coverage	%
75414	17400	200, 87	float32	transmission	*
145014	17400	200, 87	float32	transmission_uncertainty	*
145214	200	200	bool	interpolated_data	*

Appendix C. SAGE III/ISS Level 2 Solar Species Products

Table C1. Binary File Format Sheet: SAGE III/ISS Level 2 Solar Species Product

End Byte	Num Values	Dimension	Data Type	Product	Unit
3	3	3	str	mission_id	*
19	16	16	str	product_id	*
35	16	16	str	product_version	*
47	12	12	str	event_id	*
49	2	2	str	spacecraft_event_type	*
51	2	2	str	ground_event_type	*
67	16	16	str	datetime	*
75	1	1	float64	year_fraction	*
79	1	1	int32	int32_fill	*
83	1	1	float32	float32_fill	*
91	1	1	float64	float64_fill	*
95	1	1	float32	latitude	degrees
99	1	1	float32	longitude	degrees
103	1	1	float32	solar_beta	degrees
107	1	1	int32	n_ground_track_altitudes	*
151	11	11	float32	ground_track_altitude	km
327	176	176	str	ground_track_datetime	*
371	11	11	float32	ground_track_latitude	degrees
415	11	11	float32	ground_track_longitude	degrees
459	11	11	float32	ground_track_ray_direction	degrees
503	11	11	float32	spacecraft_latitude	degrees
547	11	11	float32	spacecraft_longitude	degrees
591	11	11	float32	spacecraft_altitude	km
595	1	1	int32	n_altitudes	*
1395	200	200	float32	altitude	km
2195	200	200	float32	geopotential_altitude	km

2196	1	1	bool	contamination_door_closed	*
2197	1	1	bool	solar_eclipse	*
2198	1	1	bool	hexapod_error	*
2199	1	1	bool	nadir_drift	*
2200	1	1	bool	time_questionable	*
2201	1	1	bool	exoatmospheric_blockage	*
2202	1	1	bool	exoatmospheric_disturbance	*
2203	1	1	bool	thermal_control_fault	*
2204	1	1	bool	ephemeris_gaps	*
2404	200	200	bool	disturbance	*
2405	1	1	bool	disturbance_correction	*
2409	1	1	int32	ccd_version	*
2410	1	1	bool	wavelength_calibration	*
2414	1	1	float32	ccd_temperature	deg C
2418	1	1	float32	ccd_temperature_deviation	deg C
2422	1	1	float32	ccd_shield_temperature	deg C
2426	1	1	float32	spectrometer_zenith_temperature	deg C
2458	32	32	str	climatology_source	*
2490	32	32	str	met_source	*
3290	200	200	float32	temperature	K
4090	200	200	float32	pressure	hPa
4890	200	200	float32	neutral_density	cm^{-3}
5090	200	200	bool	climatology_used	*
5094	1	1	float32	tropopause_altitude	km
5098	1	1	float32	tropopause_pressure	hPa
5102	1	1	float32	tropopause_temperature	K
5106	1	1	float32	sunspot_coverage	%
5306	200	200	bool	interpolated_data	*
6106	200	200	float32	o3_ao3	cm^{-3}
6906	200	200	float32	o3_ao3_uncertainty	cm^{-3}

7706	200	200	float32	o3_mlr	cm^{-3}
8506	200	200	float32	o3_mlr_uncertainty	cm^{-3}
9306	200	200	float32	o3_mes	cm^{-3}
10106	200	200	float32	o3_mes_uncertainty	cm^{-3}
10906	200	200	float32	h2o	cm^{-3}
11706	200	200	float32	h2o_uncertainty	cm^{-3}
12506	200	200	float32	no2	cm^{-3}
13306	200	200	float32	no2_uncertainty	cm^{-3}
13310	1	1	int32	n_aerosol_channels	*
13346	9	9	float32	aerosol_wavelength	nm
13382	9	9	int32	nominal_aerosol_wavelength	nm
20582	1800	200, 9	float32	aerosol_extinction	km^{-1}
27782	1800	200, 9	float32	aerosol_extinction_uncertainty	km^{-1}
27818	9	9	float32	stratospheric_aerosol_optical_depth	*
27854	9	9	float32	stratospheric_aerosol_optical_depth_uncertainty	*
27890	9	9	float32	rayleigh_cross_section	cm^3/km
28690	200	200	float32	o3	cm^{-3}
29490	200	200	float32	o3_uncertainty	cm^{-3}
36690	1800	200, 9	int32	derived_aerosol_flag	*
36694	1	1	float32	aerosol_tropopause_height	Km
36758	64	64	str	aerosol_flag_doi	*
37558	200	200	float32	mode_radius_p5	nm
38358	200	200	float32	mode_radius_p95	nm
39158	200	200	float32	mode_radius_median	nm
39958	200	200	float32	mode_radius_mad	nm
40758	200	200	float32	distribution_width_p5	*
41558	200	200	float32	distribution_width_p95	*
42358	200	200	float32	distribution_width_median	*
43158	200	200	float32	distribution_width_mad	*

43958	200	200	float32	surface_area_density_p5	um^2 cm^{-3}
44758	200	200	float32	surface_area_density_p95	um^2 cm^{-3}
45558	200	200	float32	surface_area_density_median	um^2 cm^{-3}
46358	200	200	float32	surface_area_density_mad	um^2 cm^{-3}
47158	200	200	float32	volume_density_p5	um^3 cm^{-3}
47958	200	200	float32	volume_density_p95	um^3 cm^{-3}
48758	200	200	float32	volume_density_median	um^3 cm^{-3}
49558	200	200	float32	volume_density_mad	um^3 cm^{-3}
50358	200	200	float32	number_density_p5	cm^{-1}
51158	200	200	float32	number_density_p95	cm^{-1}
51958	200	200	float32	number_density_median	cm^{-1}
52758	200	200	float32	number_density_mad	cm^{-1}
53558	200	200	float32	effective_radius_p5	nm
54358	200	200	float32	effective_radius_p95	nm
55158	200	200	float32	effective_radius_median	nm
55958	200	200	float32	effective_radius_mad	nm

Appendix D. SAGE III/ISS Level 2 Lunar Species Products

Table D1. Binary File Format Sheet: SAGE III/ISS Level 2 Lunar Species Product

End Byte	Num Values	Dimension	Data Type	Product	Unit
3	3	3	str	mission_id	*
19	16	16	str	product_id	*
35	16	16	str	product_version	*
47	12	12	str	event_id	*
49	2	2	str	spacecraft_event_type	*
51	2	2	str	ground_event_type	*
67	16	16	str	datetime	*
75	1	1	float64	year_fraction	*
79	1	1	int32	int32_fill	*
83	1	1	float32	float32_fill	*
91	1	1	float64	float64_fill	*
95	1	1	float32	latitude	degrees
99	1	1	float32	longitude	degrees
103	1	1	float32	lunar_beta	degrees
107	1	1	float32	lunar_phase	*
111	1	1	float32	solar_zenith	degrees
115	1	1	int32	n_ground_track_altitudes	*
159	11	11	float32	ground_track_altitude	km
335	176	176	str	ground_track_datetime	*
379	11	11	float32	ground_track_latitude	degrees
423	11	11	float32	ground_track_longitude	degrees
467	11	11	float32	ground_track_ray_direction	degrees
511	11	11	float32	spacecraft_latitude	degrees
555	11	11	float32	spacecraft_longitude	degrees
599	11	11	float32	spacecraft_altitude	km
603	1	1	int32	n_altitudes	*

1403	200	200	float32	altitude	km
2203	200	200	float32	geopotential_altitude	km
2204	1	1	bool	contamination_door_closed	*
2205	1	1	bool	hexapod_error	*
2206	1	1	bool	nadir_drift	*
2207	1	1	bool	time_questionable	*
2208	1	1	bool	thermal_control_fault	*
2209	1	1	bool	ephemeris_gaps	*
2213	1	1	int32	ccd_version	*
2214	1	1	bool	wavelength_calibration	*
2218	1	1	float32	ccd_temperature	deg C
2222	1	1	float32	ccd_temperature_deviation	deg C
2226	1	1	float32	ccd_shield_temperature	deg C
2230	1	1	float32	spectrometer_zenith_temperature	deg C
2262	32	32	str	climatology_source	*
2294	32	32	str	met_source	*
3094	200	200	float32	temperature	K
3894	200	200	float32	pressure	hPa
4694	200	200	float32	neutral_density	cm^{-3}
4894	200	200	bool	climatology_used	*
4898	1	1	float32	tropopause_altitude	km
4902	1	1	float32	tropopause_pressure	hPa
4906	1	1	float32	tropopause_temperature	K
4910	1	1	float32	altitude_adjustment	Km
5710	200	200	float32	o3	cm^{-3}
6510	200	200	float32	o3_uncertainty	cm^{-3}
7310	200	200	float32	no2	cm^{-3}
8110	200	200	float32	no2_uncertainty	cm^{-3}
8910	200	200	float32	no3	cm^{-3}
9710	200	200	float32	no3_uncertainty	cm^{-3}

Appendix E. Reference Absorption Cross Sections for Gas Retrievals

Table E1. Absorption Spectrum Data Source by Species

Gas Species	Source
Ozone	Gorshelev/Serdyuchenko 2014 (Gorshelev, Serdychenko, Weber, Chehade, Burrows)
Nitrogen Dioxide	SCIAMACHY NO_2 Version 1.0, Aug. 2000 (Bogumil, Orphal and Homann)
Nitrogen Trioxide	Yokelson 1994 (Yokelson, Burkholder and Fox)
Water Vapor	HITRAN 2004 (Rothman, Jacquemart and Barbe)
Chlorine Dioxide	SCIAMACHY OClO Version 1.0, Aug. 2000 (Bogumil, Orphal and Homann)
Dioxygen	HITRAN 2004 (Rothman, Jacquemart and Barbe)
Tetraoxygen	Greenblatt 1990 (Greenblatt, Orlando and Burkholder)
Rayleigh-Scattering	Bucholtz 1995 (Bucholtz)